

Beyond the Solid Raft: Geometric Strategies to Prevent Build Plate Bowing In CuCrZr L-PBF

Andrei-Alexandru Popa*, Andrew Seltzman†, Sebastian Leon Lasowy*, Erick Liang†, F. N. Depboylu*

* Institute of Mechanical and Electrical Engineering (IME), SDU Mechatronics (Centre of Industrial
Mechanics), University of Southern Denmark, DK-6400, Sønderborg, Denmark

† Plasma Science and Fusion Center (PSFC), Massachusetts Institute of Technology, Cambridge,
MA-02139, USA

Abstract

Build plate bowing in Laser Powder Bed Fusion (L-PBF) presents a major challenge when printing copper and its alloys, due to their high reflectivity and thermal conductivity. These conditions often cause dimensional inaccuracies and degrade structural properties—especially in large, monolithic parts for fusion applications. Fully solid rafts are commonly used to mitigate distortion, but are inefficient for large components. Standard support structures, conversely, often lead to warping, out-of-plane growth, and poor downskin quality. This study builds on prior resin-based research that showed patterned raft geometries can reduce out-of-plane deformation while maintaining support. Here, we investigate two patterned raft designs, each in two size configurations, for L-PBF CuCrZr printing. Results show that small geometric changes significantly affect print quality. Combined with variations in recoating time, unexpected improvements in upskin quality were also observed. These findings suggest that optimized raft patterning offers a promising, material-efficient strategy for large CuCrZr L-PBF.

Introduction

Build plate warping in laser powder bed fusion (L-PBF) metal additive manufacturing results primarily from coefficient of thermal expansion (CTE) mismatch-driven strains at the plate–part interface (King, et al. 2015). To guide the development of effective raft geometries, a parallel, preliminary study was conducted using vat photopolymerization (VPP) as a low-cost analogue to metal L-PBF. The purpose of this surrogate investigation was to evaluate whether the physical impact of proposed raft modifications on build plate deformation was significant enough to be detected experimentally.

In 3D printing, especially when dealing with metal additive manufacturing, the use of solid rafts often yields superior results due to the reliable thermal conductivity they provide between the part and the build plate, which helps mitigate issues such as warping or delamination (Yadroitsev, et al. 2021). From a material efficiency standpoint, however, support structures are generally preferred, as they consume less feedstock and reduce overall print time. Despite their advantages, supports can introduce complications during post-processing and may compromise dimensional accuracy or surface finish (Rott, et al. 2020). While solid rafts are technically the optimal choice for stability, they are often avoided because of practical post-processing limitations. For instance, if removal is performed using EDM wire cutting, the part can be detached at zero offset from the build plate, minimizing waste. Conversely, when using mechanical methods such as sawing, additional height must be added to the part to allow for separation, resulting in unnecessary material usage—particularly problematic if the added height serves no functional purpose. This trade-off highlights the tension between ideal printing conditions and real-world production constraints.

Rafts are also commonly employed in FFF 3D printing to mitigate warping (Ramian et al., 2021), enhance surface roughness (Demircioglu et al., 2019), and thereby improve the geometric accuracy of fabricated parts. Warping is a significant challenge in this process, arising from the rapid heating and cooling of the printed material, which generates internal stresses within the component (Syrlybayev et al., 2021). These stresses can exceed the adhesive forces between the print and the build plate, leading to deformation or print failure due to part detachment. The raft mitigates this effect by increasing the contact surface area between the build plate and the printed part, thereby enhancing adhesion (Lv et al., 2022). Unlike LPBF, the primary heat dissipation mechanism in FFF involves transfer to the surrounding ambient air rather than conduction into the build plate (Syrlybayev et al., 2021).

While VPP and metal L-PBF differ substantially in their thermomechanical behavior—VPP relies on ultraviolet (UV) light to initiate photopolymerization at room temperature with some heat released due to the exothermic nature of the reaction (Corcione et. al 2006), with shrinkage driven primarily by molecular densification (Lee, Ng and Su 2025), whereas L-PBF involves high-temperature melting, thermal contraction, and complex residual stress buildup (Bai, et al. 2022)—both processes result in differential shrinkage between the printed material and the build plate. This similarity in the outcome of warping justified the use of VPP as a rapid, cost-effective test platform.

In the VPP study, raft geometries were systematically varied in terms of shape, contact area, and lattice topology. These tests identified geometric parameters that reduced warping in the photopolymer context. However, due to the substantial differences in thermal profiles and mechanical behavior between the two processes, these specific raft designs were not directly transferred to the metal L-PBF trials. Instead, the results from the VPP experiments were used to inform the design of new raft geometries, tailored specifically to the thermal and mechanical demands of metal additive manufacturing.

This approach enabled early, rapid hypothesis testing and provided experimental feedback on the effectiveness of raft strategies before committing to resource-intensive metal printing trials. Ultimately, the study aims to establish a workflow where fast, low-cost surrogate testing using VPP can support the predictive design of support structures in metal L-PBF, accelerating the path from concept to functional mitigation strategies. While the direct correlation between build plate warping in VPP versus L-PBF falls outside the scope of the current effort, similarities between the impact of the two manufacturing techniques have been successfully identified empirically.

Materials and Methods

To identify a geometry effective in mitigating build plate warping, a series of test coupons with varying raft designs were fabricated. A preliminary resin-based study presented lattice-based raft structures designed and tested using stereolithography (SLA) printing. A parametric sweep of design variables was performed to assess the impact of fully self-supporting raft structures on mitigating build plate warping. The study aimed to characterize the mechanical response of these support structures due to the layer-by-layer photopolymer curing process and establish a framework for understanding raft design principles in other additive manufacturing processes, such as LPBF. The experimental study tested several raft structures printed beneath solid rectangular blocks of resin on detachable magnetic build plates (Reference source not found.). The spring steel buildplate flexes due to the misfit stresses, enabling post-process removal and measurements of the build plate (Reference source not found.). Measurements of height and curvature were performed along the center of the build plate using a coordinate measurement machine (CMM) (Reference source not found.).

Several shapes and dimensions of lattice units, and intersecting patterns were tested. The study found that among tested design parameters, bottom contact area of the supports with the build plate had the most significant effect on raft structure performance. A smaller contact area lowered contact stress, but also reduced overall mechanical support. Another effect the study hypothesized was that a gradual intersection compared to a simultaneous and uniform intersection of lattice elements during the build process would reduce the stresses accumulated at the build plate. While the effect was not demonstrated in the resin study (**Figure 8**), the comparison between hexagon-trapezoid and pentagon wall geometries aim to assess whether intersection pattern has an effect on support structure performance in L-PBF.

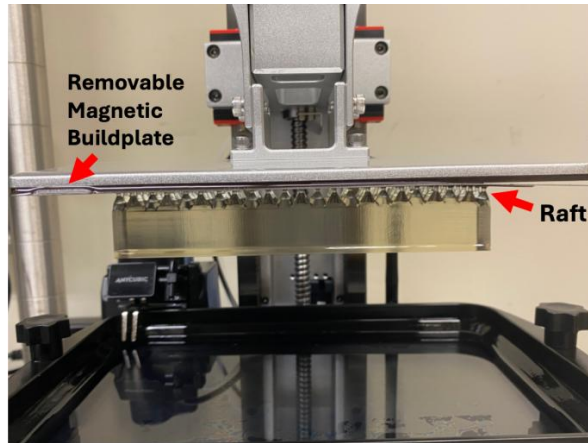


Figure 1 - An AnyCubic Photon M3 Plus Resin 3D printer tested raft designs supporting a solid test block in clear resin of volume 170 x 30.1 x 1.5 mm.; the magnetic adhesive base and flexible magnetic build plate were detached and measured, with rafts including a 12mm brim to prevent delamination

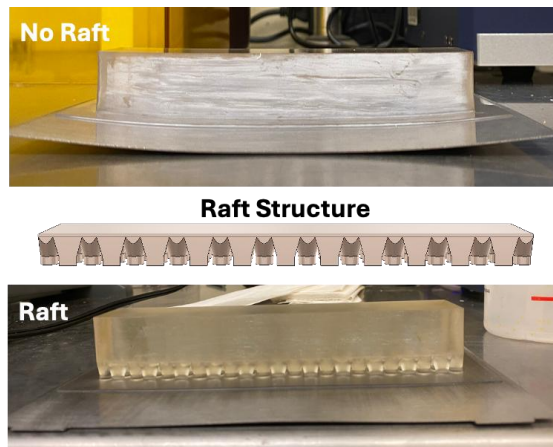


Figure 2 - Lattice-based raft structures with varying parameters including height, density, bottom and top contact area, were tested beneath solid blocks of resin.; the magnetic build plate was detached and measured before separation of the block and raft structure

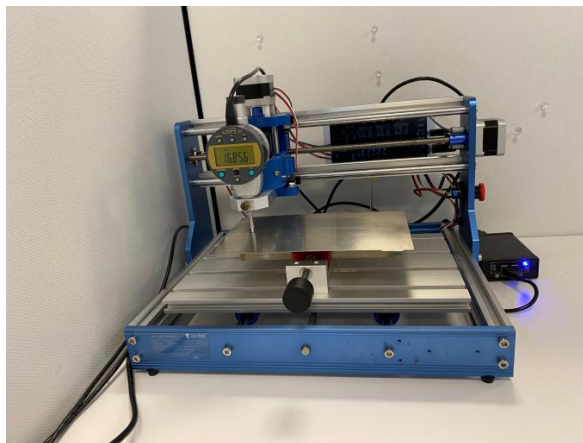
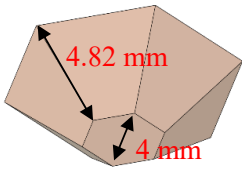
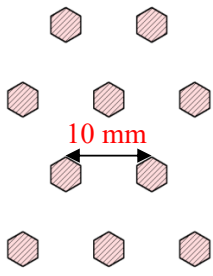
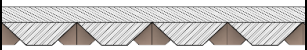

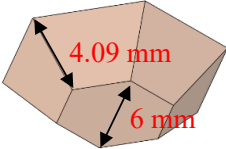
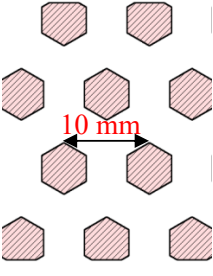
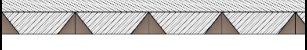
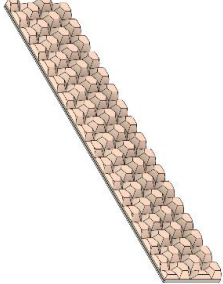
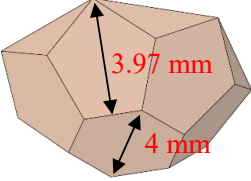
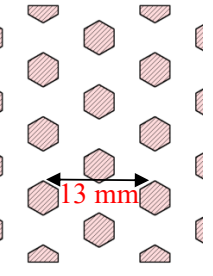
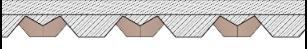
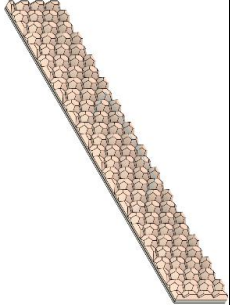


Figure 3 - A coordinate measurement machine measures height along the center of a detached buildplate. Curvature is calculated from a circle fitted onto the smoothed and median filtered profile data

The methods were mirrored for the L-PBF study. Each coupon comprised a $170 \times 19.5 \times 2$ mm rectangular component printed atop a distinct raft structure. The narrower width is chosen out of material-saving considerations and deemed reasonable by the hypothesis that the inherent temperatures of the L-PBF process would cause significant build plate bowing even for smaller build envelopes. Six different raft geometries were evaluated in this study. The first two, hereafter referred to as “Solid 3mm” and “Solid 5mm,” were fully solid rafts with outlines matching the footprint of the part and thicknesses of 3 mm and 5 mm, respectively. As the “T” series depicts hexagon-based stumps with trapezoidal walls, the pentagonal-walled samples are denoted by the “P” series. The remaining four geometries employed a lattice design composed of repeated hexagonal-based 10 mm segments. Details of the lattice configurations, including views of individual segments, are provided in Figure 4 and Figure 5.

Designator		Raft element	Build plate surface	Side View	3D View
R2 T	2mm Base Hexagon, Trapezoid Walls				
R3 T	3mm Base Hexagon, Trapezoid Walls				
R2 P	2mm Base Hexagon, Pentagon Walls				

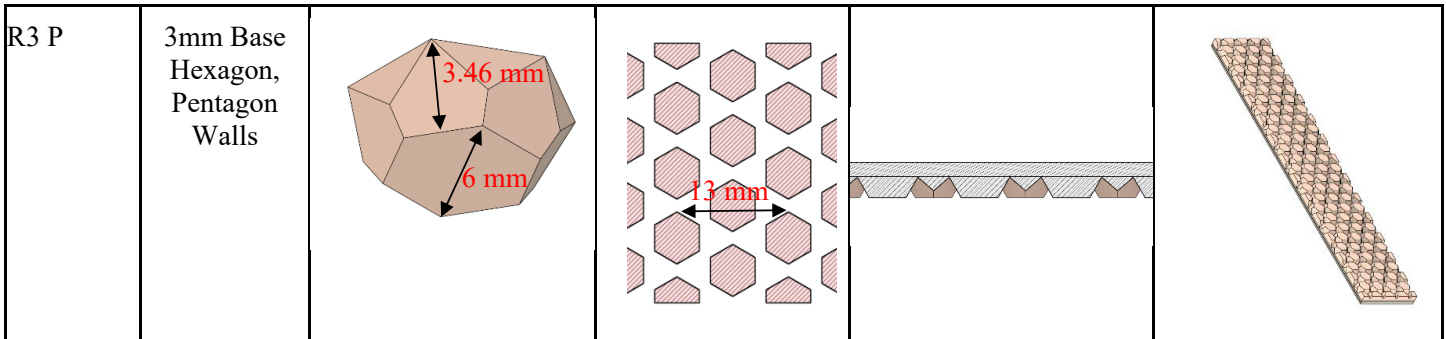


Figure 4 – Tested geometry details

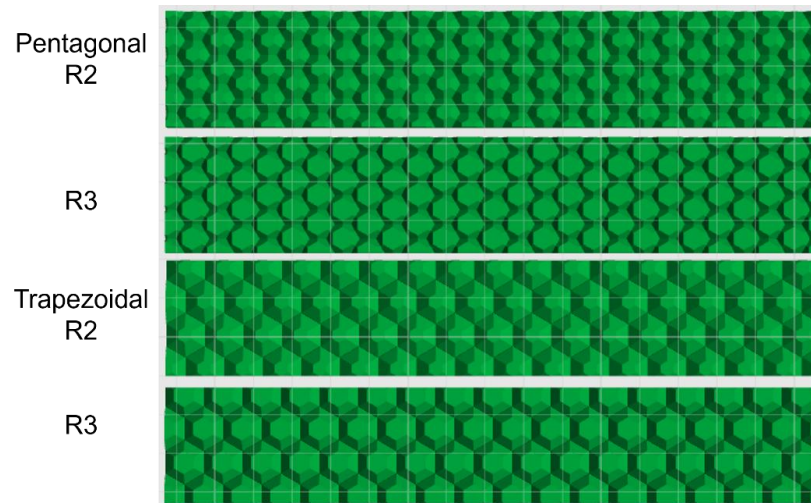


Figure 5 - bottom view of rafts

The parts were printed using Osprey C18150 copper powder, produced by Sandvik, with a particle size distribution of 15–53 μm . This alloy, when processed via Laser Powder Bed Fusion (L-PBF), exhibits a yield strength of 160 MPa, a tensile strength of 210 MPa, and an elongation at break of 40% (Sandvik 2025). All prints were carried out using the following fixed parameters:

- Laser power: 378 W
- Scanning speed: 632 mm/s
- Laser spot size: 100 μm
- Hatch spacing: 0.13 mm

The only variable parameter across the builds was the recoater delay—a brief pause introduced after the deposition of each layer to protect the laser optics from overheating. Most prints employed a 10-second recoater delay, while two were produced with a 0-second delay to observe the differences.

To quantify the results obtained from these tests and seeking to improve on the original measurement device, a custom built CMM (Figure 6) was used to measure the shape of the build plates, before and after printing. Data was collected on the non-printed-upon, underside surface of the plates.

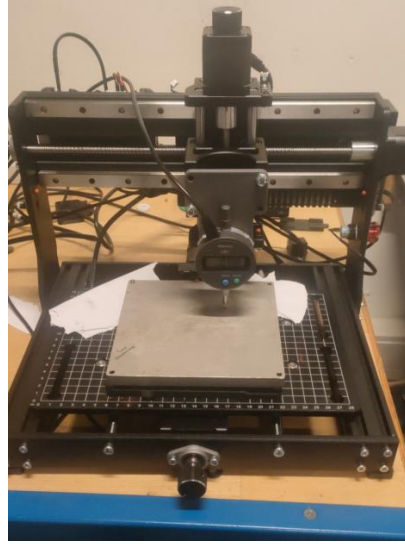


Figure 6: CMM used for plate measurements

The CMM setup consisted of a modified CNC machine with a digital dial indicator (Mitutoyo ID-S112Xb2) mounted in place of the spindle. To validate the accuracy of the setup, a known-flat plate was measured along the X and Y axes. The measurement results are presented in Figure 7.

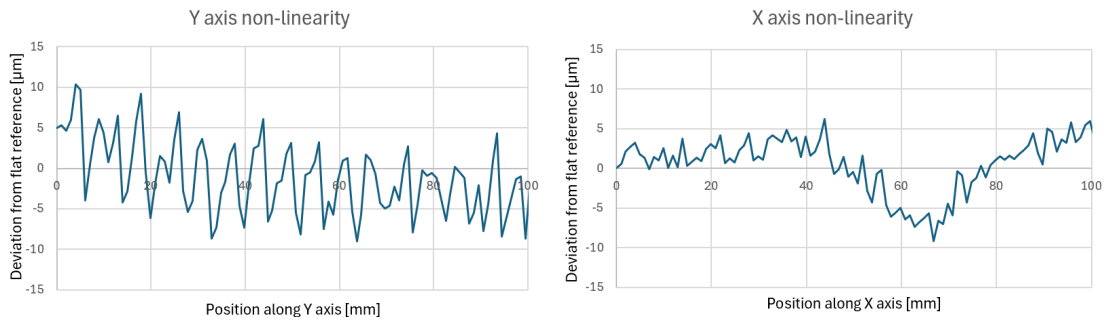


Figure 7: Deviation from flat plane along Y (left) and X (right) axes of the CMM

While these measurements show some nonlinearity, it is an order of magnitude lower than the values of the curvature measured in the build plates.

Two types of measurements were performed. The first was a 20x20 grid of samples across the entire surface of the build plate. This was repeated 3 times for each plate and resulted in a 3D cloud of 1200 points lying on each sample, to which a surface was fitted for visualization purposes.

The second type of measurement was performed by collecting the heights of 100 points lying on the diagonal of the plate aligned with the major dimension of the print. This was repeated 3 times for each plate, resulting in a total of 300 points per plate. A parabolic function of the form $y = ax^2 + bx + c$ was subsequently fitted to these data points using the least-squares method. Bending was quantified by taking the difference between the “a” parameter of the post-print and pre-print measurements.

Results and Discussion

The results of the resin study indicated a notable effect of the rafts on the bowing of the build plate, with the fitted results highlighting their positive influence as per Figure 8.

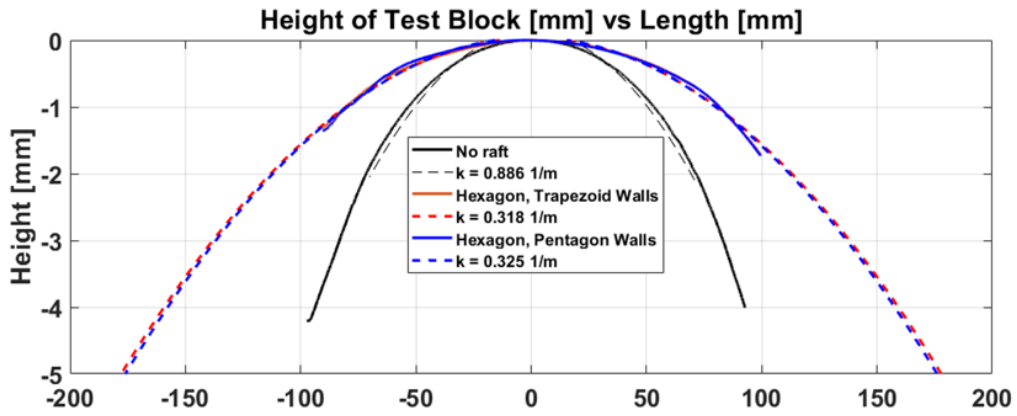
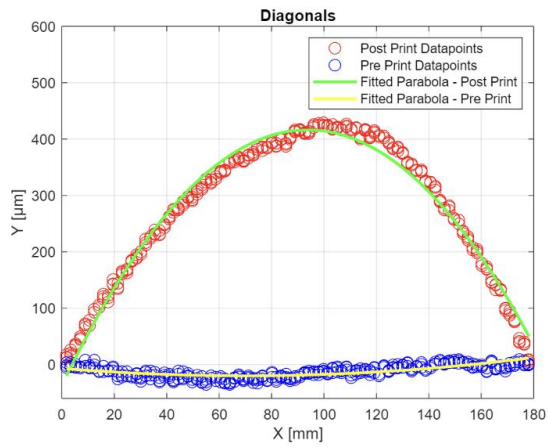


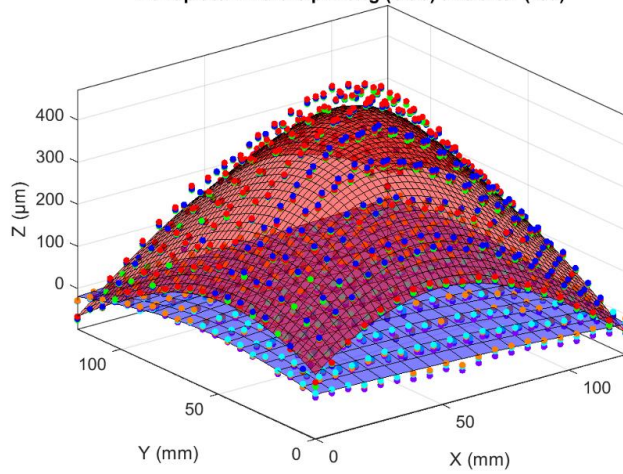
Figure 8. Height profile data and circular fits plotted along the length of a detached build plate for no raft, and hexagon trapezoid and pentagon wall scenarios. The x and y intercepts were defined to be the center of the curvature around its highest point.

In the L-PBF case, a 3D mapping of points was performed, as show in Figure 9.

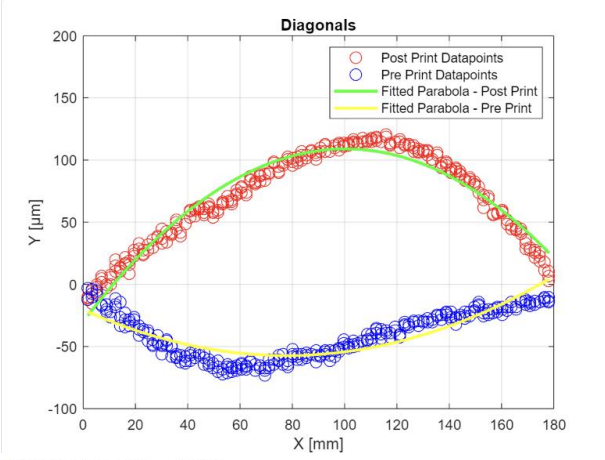
Buildplate_pre_curve = 0.0027
 Buildplate_post_curve = -0.0514



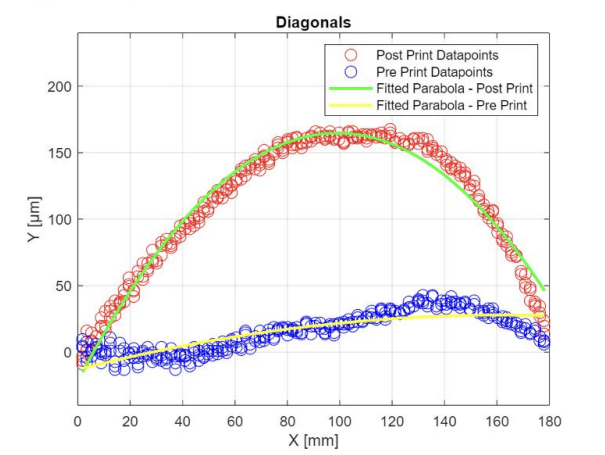
Buildplate 4 Before printing (blue) and after (red)



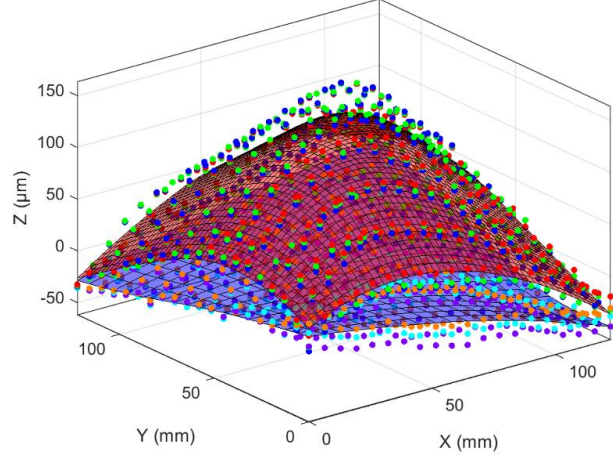
Buildplate_pre_curve = 0.0061
 Buildplate_post_curve = -0.0138



Buildplate_pre_curve = -0.0015
 Buildplate_post_curve = -0.0190



Buildplate 5 Before printing (blue) and after (red)



Buildplate 9 Before printing (blue) and after (red)

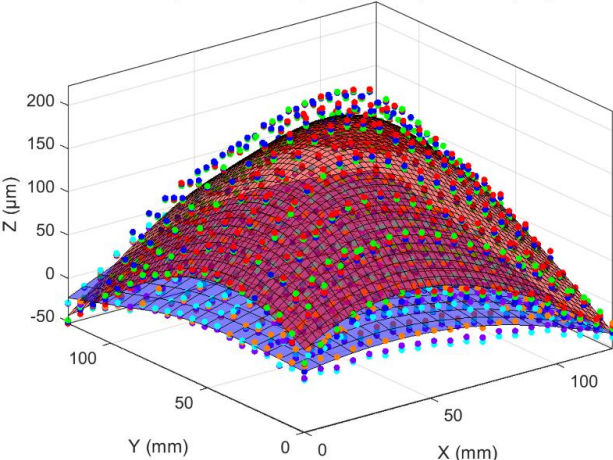


Figure 9 - 3D point mapping of bowing, for 5mm solid raft (top), R3P (middle) and R2T (bottom)

After the samples were measured, the curvature changes for different raft geometries were compared. The comparative results for the samples printed with the 10 second recoating delay time can be seen in Figure 10.

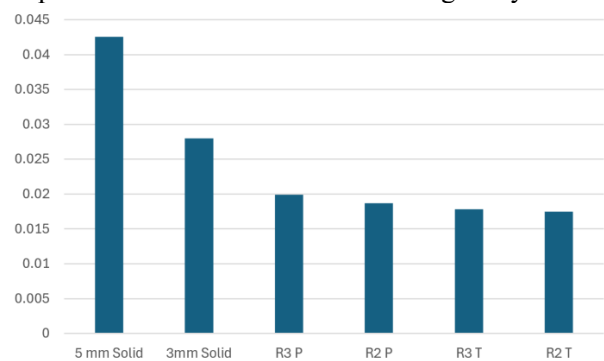


Figure 10 - average deviation in curvature

It was observed that the addition of any non-solid raft geometry reduced the severity of deformation significantly compared to the solid rafts. Considering this curvature mitigation parameter, the performance of the various non-solid geometries was similar, with the “T” raft type slightly outperforming the “P” rafts. A larger

difference between the raft geometries can be observed when visually inspecting the printed samples. As seen in Figure 11, the samples that use the “T” type of rafts exhibited printing defects, while the “P” prints did not.



Figure 11: From top: Solid 3 mm, Solid 5 mm, R3 T, R3 P, R2 T, and R3 P

The effect of the recoater delay on the curvature was also significant. The average of the curvature change indicator of the “T” type samples printed with no recoater delay was found to be 0.0556, in comparison to 0.0177- the same metric found for their equivalents printed with a manufacturer-recommended 10 second recoater delay. This result is likely attributed to a higher thermal stress being generated in the parts printed with a shorter or no delay. The longer pause between printing layers enables the thermal energy generated by the printing process to be, in part, dissipated into the surrounding environment. This decreases the buildup of thermal stresses, resulting in a less significant deformation.

Moreover, despite the positive influence of the non-solid rafts, the “P” sets exhibited a deteriorated top surface relative to both the solid and the “T” samples. The change in cross-section in the raft struts can be linked to upskin quality, likely due to the magnitude of overlap between adjacent struts. Moreover, the defects are amplified by the out of plane growth leading to inhomogeneity in powder redistribution, resulting in inferior melt pool quality.

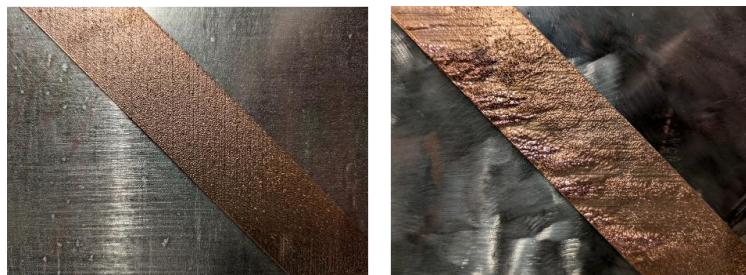


Figure 12 - Surface quality on trapezoidal wall (left) and pentagonal wall (right) coupons, with defects visible on the latter

The bowing effect is linked to the manufacturing of and maintained contact between the part and the build plate. After removing the printed CuCrZr part from the buildplate, a significant decrease in curvature can be observed – as seen in Figure 13.

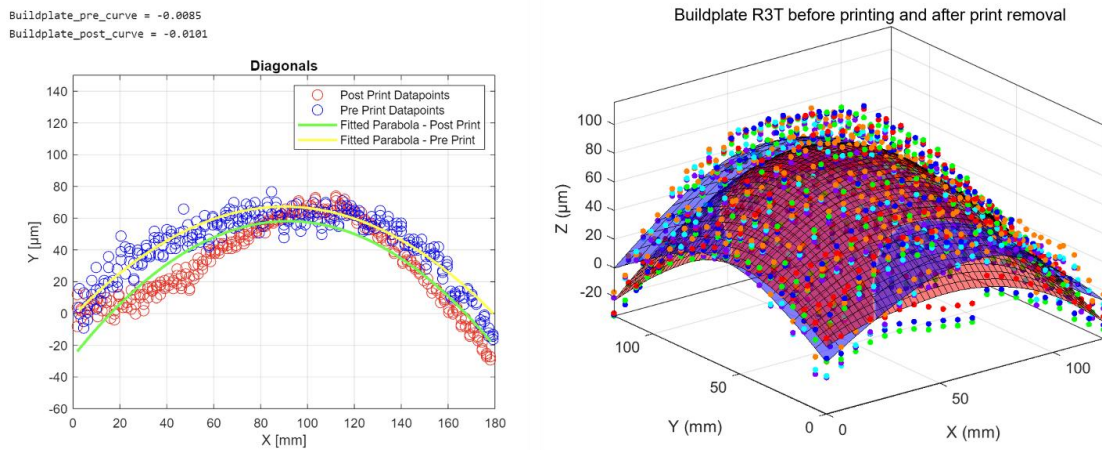


Figure 13 - Build plate bowing pre-print (yellow) and post-print, with part removed (green)

Conclusion

This study demonstrates that patterned raft geometries offer a significant advantage over conventional solid rafts in minimizing build plate bowing during L-PBF of CuCrZr. Both the "T" and "P" patterns improved dimensional stability compared to fully solid rafts, with the "T" design showing superior performance in reducing warping and maintaining part flatness. The influence of raft base radius was non-negligible, indicating that even minor geometric adjustments can critically impact print outcomes. Additionally, an optimized recoating time—saturating at approximately 10 seconds—was found to enhance upskin quality, further contributing to part integrity. Surface roughness analysis revealed that the "P" design consistently exhibited inferior results, including more pronounced out-of-plane growth, underscoring the importance of raft pattern selection not only for mechanical stability but also for surface fidelity. Altogether, these findings support the use of structured, material-efficient rafts as a viable strategy for large-scale copper alloy additive manufacturing, particularly in applications where precision and stability are paramount.

Acknowledgement

We would like to acknowledge Olgierd Nowakowski for his help with manufacturing the components.

References

- J. Ramian, J. Ramian, and D. Dziob, "Thermal Deformations of Thermoplast during 3D Printing: Warping in the Case of ABS," *Materials*, vol. 14, no. 22, Art. no. 7070, 2021
- Demircioglu, Pinar & Bogrekcı, Ismail & Sucuoglu, Hilmi & Gultekin, Asli. . The Effect of Contact and the Raft on the Surface Roughness of 3D Printed Object., 2019
- K. Singh, "Experimental study to prevent the warping of 3D models in fused deposition modeling," *International journal of plastics technology*, vol. 22, no. 1, pp. 177–184, 2018
- Syrlybayev, D.; Zharylkassyn, B.; Seisekulova, A.; Perveen, A.; Talamona, D. Optimization of the Warpage of Fused Deposition Modeling Parts Using Finite Element Method. *Polymers*, 2021

- N. Lv, Y. Li, and Y. Qiao, "Generation Algorithm of a Novel Platform Attached Support Structure for FDM-Fused Deposition Modeling," *Advances in materials science and engineering*, vol. 2022, Art. no. 1532924, 2022
- Corcione CE, Greco A, Maffezzoli A. Temperature evolution during stereolithography building with a commercial epoxy resin. *Polymer engineering and science*. 2006
- Bai, Yuchao, Cuiling Zhao, Jiayi Zhang, and Hao Wang. 2022. "Abnormal thermal expansion behaviour and phase transition of laser powder bed fusion maraging steel with different thermal histories during continuous heating." *Additive Manufacturing*.
- King, W. E., A. T. Anderson, R. M. Ferencz, N. E. Hodge, C. Kamath, S. A. Khairallah, and A. M. Mon and Rubencik. 2015. "Laser powder bed fusion additive manufacturing of metals; physics, computational, and materials challenges." *Applied Physics Review* 041304
- Lee, Taehyub, Chin Siang Ng, and Pei-Chen Su. 2025. "Warpage correction for vat photopolymerization 3D printing." *Additive manufacturing*.
- Rott, Sebastian, Alexander Ladewig, Friedberger Katrin, Johannes Casper, Moritz Full, and Johannes Henrich Schelifenbaum. 2020. "Surface roughness in laser powder bed fusion – Interdependency of surface orientation and laser incidence." *Additive Manufacturing*.
- Sandvik. 2025. "Sandvik Osprey® C18150 Datasheet." 04 06. <https://www.metalpowder.sandvik/en/products/metal-powder-alloys/copper-alloys/osprey-c18150/?html-to-pdf=true>.
- Yadroitsev, Igor, Ina Yadroitsava, Anton Du Plessis, and Eric MacDonald. 2021. *Fundamentals of Laser Powder Bed Fusion of Metals (Additive Manufacturing Materials and Technologies)*. Elsevier.